

Quantum Entanglement and Modulation Enhancement of Free-Electron–Bound-Electron Interaction

Zhexin Zhao,¹ Xiao-Qi Sun,^{2,3,*} and Shanhui Fan^{1,†}

¹Department of Electrical Engineering, Ginzton Laboratory, Stanford University, Stanford, California 94305, USA

²Department of Physics, McCullough Building, Stanford University, Stanford, California 94305, USA

³Department of Physics, Institute for Condensed Matter Theory, University of Illinois at Urbana-Champaign, Illinois 61801, USA



(Received 21 October 2020; accepted 19 March 2021; published 11 June 2021)

The modulation and engineering of the free-electron wave function bring new ingredients to the electron-matter interaction. We consider the dynamics of a free-electron passing by a two-level system fully quantum mechanically and study the enhancement of interaction from the modulation of the free-electron wave function. In the presence of resonant modulation of the free-electron wave function, we show that the electron energy loss and gain spectrum is greatly enhanced for a coherent initial state of the two-level system. Thus, a modulated electron can function as a probe of the atomic coherence. We further find that distantly separated two-level atoms can be entangled through interacting with the same free electron. Effects of modulation-induced enhancement can also be observed using a dilute beam of modulated electrons.

DOI: 10.1103/PhysRevLett.126.233402

Introduction.—The interactions of free electrons with matters have provided a number of technologies for the study of material and photonic systems [1–4]. Among these technologies, electron energy loss spectroscopy (EELS) probes the excitation spectrum of the matter [1–3,5–7], and photo-induced near-field electron microscopy (PINEM) detects the near-field of nanostructures under optical pumping [8–15]. Moreover, in recent years, the quantum nature of the free electron has attracted considerable research interest [3,4,8–23]. In particular, over the last decade, engineering the quantum states of the free electron becomes possible. For example, experiments demonstrated the modulation of a single electron wave function by ultrafast laser technique [8–18].

With the capability of wave function engineering, it is crucial to investigate how such quantum engineering can be used to enhance and tailor electron-material interaction and to create new functionalities. Studies have shown increased scattering cross section, and coherent control of atomic transitions using a resonant modulated electron beam [24–26]. Entanglement between electron and photons has been studied in the interaction of an electron with an optical cavity [27]. Moreover, recently Gover and Yariv has studied the interaction of a modulated electron beam and an atom, in a semiclassical formalism, and showed the possibilities of Rabi oscillation in such free-electron–bound-electron interaction [25].

In this Letter, we apply a fully quantum scattering matrix description to the free-electron–bound-electron interaction [2,3,15,26,28]. We investigate the electron energy loss and gain spectrum and the perturbation on the density matrix of the two-level system, highlighting the enhancement of the

interaction resulted from the modulation of the free electron. We find the potential of probing the coherence of the two-level system using the modulated free electron. The quantum treatment also predicts the possibility of using multiple scattering processes to generate entanglement between two bound-state electrons. Finally, we consider the interaction between the two-level system and a dilute beam of modulated electrons. We discuss a possible partially mixed steady state of the atom due to the modulation, while also providing a rigorous foundation for the semiclassical results of the Rabi oscillation of the two-level system [25].

Model setup.—We consider the scattering problem between a free electron with a two-level system from first principles (Fig. 1). In the low-velocity limit, the electrons are governed by the Schrödinger equation and the interaction potential is the Coulomb potential. In analyzing the Coulomb interaction, we consider only the interaction

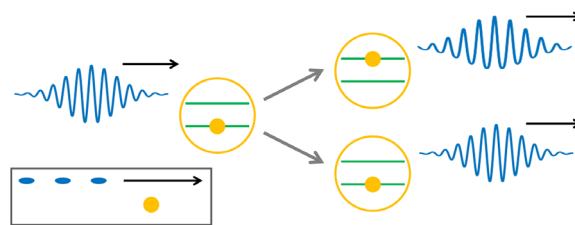


FIG. 1. Schematic of the interaction between an electron (blue wave packet) and a two-level system (orange circle). The inset shows a schematic of a train of electrons interacting with the two-level atom.

between the free electron and the bound electron, and use the dipole approximation. If we further assume that the transverse distribution of the free-electron wave function is unchanged, the model Hamiltonian becomes

$$H = \sum_{\alpha} E_{\alpha} c_{\alpha}^{\dagger} c_{\alpha} + \sum_k E_k^{\text{free}} c_k^{\dagger} c_k + \sum_q b_q [g_{21}(q) \sigma^+ + g_{12}(q) \sigma^-], \quad (1)$$

where $\alpha = 1, 2$ represents the bound states of the two-level system, c^{\dagger} and c are the creation and annihilation operators, $\sigma^+ = c_2^{\dagger} c_1$, $\sigma^- = c_1^{\dagger} c_2$, and b is the electron ladder operator $b_q = \sum_k c_{k-q}^{\dagger} c_k$ [11,27]. The coupling between the free electron and the bound state electron (g_{ij}) can be generally derived from the Coulomb interaction (Supplemental Material, Sec. I [29]).

We treat the free-electron–bound-electron scattering problem perturbatively, since the interaction is generically weak. Under the weak coupling assumption, only the electron ladder operator with $q = \omega_a/v_0$ matches the two-level system transition and contributes to the scattering. Here, ω_a is the transition frequency of the two-level system and v_0 is the velocity of the electron wave packet. In the following, we consider only such matched electron ladder operator and omit the subscript q . To second order in the dimensionless coupling coefficient g , which is proportional to $g_{21}(\omega_a/v_0)$, the scattering matrix is [29]

$$S \approx \left(1 - \frac{1}{2}|g|^2\right) I - i(gb\sigma^+ + g^*b^{\dagger}\sigma^-), \quad (2)$$

where I is the identity operator. The magnitude of the coupling (g) depends on the transition dipole moment, the free electron velocity, and the transverse distance. A typical value is $|g| \sim 10^{-3}$. An estimation for the tin-vacancy (SnV) [35,36] is in Supplemental Material, Sec. II [29]. This concise scattering matrix [Eq. (2)] provides a fully quantum mechanical description of the interaction between the free electron and the two-level system. It manifests the entanglement between the atomic transition of the bound electron and the hopping on the energy ladder of the free electron. It works well for arbitrary initial states and reveals results due to free-electron modulation that are obscured in previous studies.

Modulation of the free electron.—We briefly revisit the free-electron energy modulation and wave function engineering [11]. In PINEM, the free electron interacts with the near-field and absorbs or emits integer number of photons. The free-electron wave function with small initial energy spread then contains multiple energy components. The multiple energy levels are on a ladder with energy separation equal to the absorbed or emitted photon energy $\hbar\omega$ (Fig. 2). The unitless modulation strength g_m is defined as $g_m = e \int dz \exp(-i\omega z/v_0) E_{mz}(z)/2\hbar\omega$, where z is the

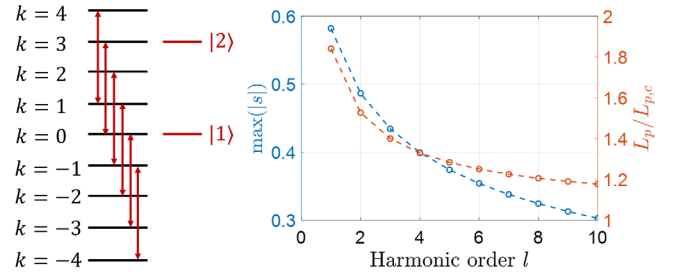


FIG. 2. Left: Schematic of the electron ladder for an electron modulated at frequency ω and the energy levels of the two-level system, where $\omega_a = l\omega$ and $l = 3$. Right: Maximal $|s|$ and the corresponding drift length for different harmonic orders.

electron propagation direction and E_{mz} is the z component of the modulation field. In the free-drift region after the energy modulation, different energy components accumulate different additional phases and the real-space electron probability distribution forms a train of microbunches [11]. Such free electron with engineered wave function is referred to as the modulated free electron in this study.

Perturbation on the two-level system.—The modulated free electron can drive the transition of the two-level system coherently. The change in the density matrix of the two-level system is obtained by tracing out the free electron state, $\Delta\rho_a = \text{Tr}_e(S\rho_{ea}^i S^{\dagger} - \rho_{ea}^i)$, where the initial density matrix $\rho_{ea}^i = \rho_e^i \otimes \rho_a^i$. In terms of the two-level system density matrix elements, we get

$$\Delta \begin{pmatrix} \rho_{a11} \\ \rho_{a22} \\ \rho_{a12} \\ \rho_{a21} \end{pmatrix} = -iM \begin{pmatrix} \rho_{a11} \\ \rho_{a22} \\ \rho_{a12} \\ \rho_{a21} \end{pmatrix}, \quad (3)$$

$$M = \begin{pmatrix} -i|g|^2 & i|g|^2 & -gs & g^*s^* \\ i|g|^2 & -i|g|^2 & gs & -g^*s^* \\ -g^*s^* & g^*s^* & -i|g|^2 & ig^{*2}s_2^* \\ gs & -gs & ig^2s_2 & -i|g|^2 \end{pmatrix},$$

where $s = \langle b \rangle$ and $s_2 = \langle b^2 \rangle$ are parameters determined by the state of the incident electron.

The lower-left off-diagonal 2×2 block of M represents the change in the atomic coherence to the first order of g , which depends strongly on the incident electron state. For a quasimonochromatic electron or a modulated electron without drift for microbunching, $s = 0$. However, for a modulated electron with a proper drift length for microbunching [11,37–39], $s \neq 0$ and may approach unity with sophisticated modulation [12,14]. Therefore, the induced coherence in the two-level atom is controlled by the modulation on the free electron.

We further study s for a modulated electron and discuss conditions to maximize $|s|$ in typical PINEM. We consider

a Gaussian electron wave packet with momentum spread $\sigma_q \ll \omega_a/v_0$. The wave packet is modulated by a laser at frequency ω , with modulation strength g_m , and propagates for a drift length L_p before it interacts with the two-level system (Supplemental Material, Sec. III [29]). We find that the magnitude of s is maximized on resonance $\omega_a = l\omega$, where the harmonic order l is an integer. Under this resonance condition,

$$|s| \approx \left| J_l \left[4|g_m| \sin \left(\frac{lL_p}{4|g_m|L_{p,c}} \right) \right] \right|, \quad (4)$$

where $L_{p,c}$ is the drift length for perfect bunching from classical analysis (Supplemental Material, Sec. III [29]). The maximal $|s|$ is the peak of Bessel function J_l and the argument gives the optimal drift length. To reach the maximal $|s|$ for the l th harmonic, the modulation strength $|g_m| > l/4$. When the modulation is strong, $|s| \approx J_l(lL_p/L_{p,c})$, the optimal drift length becomes independent of g_m . The maximal $|s|$ and the corresponding optimal drift length are shown in Fig. 2. We find that $|s|$ decreases slowly with increasing harmonic order. This trend indicates the potential to drive two-level system at high harmonics with the modulated electron [25]. The optimal drift length is larger than the drift length to create the shortest electron bunch (Fig. 2), especially for small harmonic orders.

Electron energy loss and gain spectrum.—The atomic coherence can be probed by the modulated free electron in EELS, with an enhanced signal. The change in the density matrix of the free electron is

$$\begin{aligned} \Delta\rho_e &= \text{Tr}_a(S\rho_{ea}^i S^\dagger - \rho_{ea}^i) \\ &= -|g|^2\rho_e^i + |g|^2\rho_{a11}^i b\rho_e^i b^\dagger + |g|^2\rho_{a22}^i b^\dagger\rho_e^i b \\ &\quad - i[g\rho_{a12}^i(b\rho_e^i - \rho_e^i b) + g^*\rho_{a21}^i(b^\dagger\rho_e^i - \rho_e^i b^\dagger)]. \end{aligned} \quad (5)$$

Thus, the free-electron spectrum change is $\Delta\rho_e(k) = \langle k|\Delta\rho_e|k\rangle$ (Supplemental Material, Sec. III [29]). The average energy change is

$$\begin{aligned} \langle \Delta E_e \rangle &= \hbar\omega_a |g|^2 (\rho_{a22}^i - \rho_{a11}^i) \\ &\quad + i\hbar\omega_a (g\rho_{a12}^i \langle b \rangle - g^*\rho_{a21}^i \langle b^\dagger \rangle). \end{aligned} \quad (6)$$

We find that the energy exchange between the free electron and the two-level system depends on the initial states of the two-level system and the free electron. When $\langle b \rangle \neq 0$, the electron energy loss, as well as the energy spectrum variance, is proportional to the off-diagonal elements of the two-level system density matrix to the first order in g . On the contrary, for an electron in a totally mixed state or being quasimonochromatic, $\Delta\rho_e(k)$ and $\langle \Delta E_e \rangle$ become proportional to $|g|^2$. Thus, the control of the free-electron state is crucial to observe the first order effects. In short, Eqs. (5) and (6) imply an opportunity to probe the

coherence of the two-level system by measuring the energy loss and gain spectrum of the free electron.

The enhanced EELS signal that is to the first order of g can be optimized by controlling the free-electron wave function. We discuss the optimal conditions for a typical PINEM modulated electron in Supplemental Material, Sec. IV [29]. As an demonstration, we study the free-electron spectrum change of a modulated free electron interacting with a two-level system (SnV) in a superposition state $|\Psi_a\rangle = (|0\rangle + |1\rangle)/\sqrt{2}$ (Fig. 3). We assume that the 60 keV electron is modulated at resonant frequency ω_a (620 nm) with optimal strength $g_m = 0.68$ and drift length $L_p = 10$ mm [29]. Before interacting with the two-level system, the electron spectrum is shown in Fig. 3(d), which is a typical PINEM spectrum [11]. After the interaction, the spectrum change that is proportional to $|g|$ ($|g|^2$) is plotted in Fig. 3(e) [Fig. 3(f)], where we assume a typical value $g = 1 \times 10^{-3}$. In this case, the $|g|^2$ contribution is much smaller than the $|g|$ contribution and can be neglected. The spectrum change is as Fig. 3(e). However, if either the free electron or the two-level system loses the coherence, the $|g|$ contribution disappears and the spectrum change is as Fig. 3(f). In comparison, we study a Gaussian wave packet with small initial energy spread ($\sigma_p \ll \omega_a/v_0$) [Fig. 3(a)] interacting with the same two-level system in state $|\Psi_a\rangle$. After the interaction, the spectrum change is proportional to $|g|^2$, with zero contribution proportional to $|g|$ [Figs. 3(b)–3(c)]. In contrast to typical PINEM spectra, the spectrum change probing the atomic coherence can be antisymmetric [Fig. 3(e)]. This antisymmetric part can be extracted to determine the

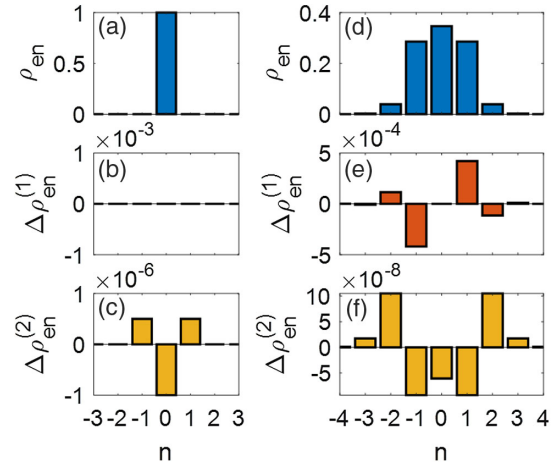


FIG. 3. Spectrum change of the free electron interacting with a two-level system in state $|\Psi_a\rangle = (|0\rangle + |1\rangle)/\sqrt{2}$, where the free electron is either a 60 keV Gaussian wave packet with $\sigma_p \ll \omega_a/v_0$ (a)–(c) or a resonant modulated wave packet with optimal modulation strength $g_m = 0.68$, modulation frequency ω_a (620 nm), and drift length 10 mm (d)–(f). (a),(d) The electron energy spectrum before the interaction. (b),(e), and (c),(f) are the spectrum changes after the interaction in the first and second order of $|g|$, respectively, where a typical $g = 1 \times 10^{-3}$ is assumed.

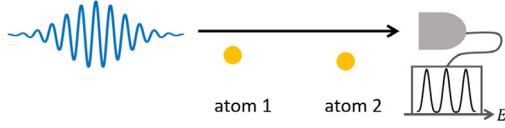


FIG. 4. Schematic of an electron interacting with two atoms.

atomic coherence experimentally (Supplemental Material, Sec. V [29]).

When the two-level system is initially at the ground state and the incident free electron has a well-defined momentum $\hbar k_0$, our result is consistent with conventional EELS [2]: $\Delta\rho_e(k) = -|g|^2\delta_{k,k_0} + |g|^2\delta_{k,k_0-\omega_a/v_0}$, which is proportional to $|g|^2$. Thus, in typical situations $|g| \ll 1$, the modulated electron provides an opportunity to probe the coherence of the two-level system with an EELS signal much stronger than the conventional EELS signal.

Entanglement.—Two separated two-level atoms can be entangled through the interaction with the same free electron. As illustrated in Fig. 4, a single electron interacts in sequence with two-level atoms 1 and 2, which have the same transition frequency ω_a . After the interactions, the electron energy is measured. We assume that the two atoms are separated enough to avoid electron wave function overlap between the two atoms. Suppose that both atoms are at the ground state and the free electron has energy spread $\sigma_q \ll \hbar\omega_a$ before the interaction, and the coupling coefficient between the electron and atom 1 (2) is g_1 (g_2). The final state after scattering is

$$|\Psi_{e12}^f\rangle = [S_2(g_2) \otimes I_1][S_1(g_1) \otimes I_2]|\Psi_e^i\rangle|\Psi_1^i\rangle|\Psi_2^i\rangle, \quad (7)$$

where S_1 (S_2) acts on the product space of the electron and atom 1 (2). We assume that when the electron interacts with one of them, the other atom has no influence. An explicit form of the final state is shown in Supplemental Material, Sec. VI [29].

After the interactions, if certain energy of the electron is measured, the two atoms are in an entangled state. For instance, when the electron has initial momentum $\hbar k$ and final momentum $\hbar k - \hbar\omega_a/v_0$, the two atoms are in the entangled state

$$\frac{1}{\sqrt{|g_1|^2 + |g_2|^2}} [g_2|\Psi_1^i\rangle(\sigma^+|\Psi_2^i\rangle) + g_1(\sigma^+|\Psi_1^i\rangle)|\Psi_2^i\rangle]. \quad (8)$$

The probability of obtaining such entangled state is $\sim(|g_1|^2 + |g_2|^2)$. It is possible to increase the coupling coefficients and hence the probability of entangled state generation by choosing two-level systems with large transition dipole moment, decreasing the distance between the electron trajectory and atoms, and decreasing the electron speed [40]. Furthermore, entanglement between multiple atoms is possible if the single electron interacts with each of them before the energy measurement.

Multiple electrons.—The enhancement of perturbation on a two-level system resulting from the free-electron resonant modulation is also manifested in the interaction between the two-level system and a dilute electron beam (inset of Fig. 1), since the atomic coherent excitation can build up in the sequential scattering of the electrons by the atom. The adjacent electrons are separate with an average separation larger than the longitudinal size of the electron wave function, such that, for each electron interacting with the two-level system, the influence of other electrons is negligible. Since the perturbation of a single free-electron interaction is given by Eq. (3), the effective dynamics of the two-level system is

$$\frac{\Delta u}{\Delta t} = -i\frac{M}{T}u - \Gamma u, \quad \Gamma = \begin{pmatrix} 0 & -\frac{1}{\tau} & 0 & 0 \\ 0 & \frac{1}{\tau} & 0 & 0 \\ 0 & 0 & \frac{1}{2\tau} & 0 \\ 0 & 0 & 0 & \frac{1}{2\tau} \end{pmatrix}, \quad (9)$$

where $u = [\rho_{a11}, \rho_{a22}, \rho_{a12}, \rho_{a21}]^T$, T is the time separation between adjacent electrons, and τ is the decay time of the two-level system [41]. The average dynamics is similar to the optical Bloch equations [26]. The effective Hamiltonian describing the two-level system driven by the electron beam is $H_{\text{eff}} = M/T - i\Gamma$. The effective Hamiltonian has a zero eigenvalue corresponding to the steady state:

$$\rho_a = \frac{1}{1 + 2\left(\frac{2|gs|\tau}{T}\right)^2} \begin{bmatrix} 1 + \left(\frac{2|gs|\tau}{T}\right)^2 & i\frac{2g^*s^*\tau}{T} \\ -i\frac{2gs\tau}{T} & \left(\frac{2|gs|\tau}{T}\right)^2 \end{bmatrix}, \quad (10)$$

where we assume $|s| \gg |g|$ due to resonant modulation. Without modulation, i.e., $s = s_2 = 0$, the steady state becomes $\rho_a = [(1)/(1 + 2|g|^2\tau/T)] \begin{bmatrix} 1 & 0 \\ 0 & |g|^2\tau/T \end{bmatrix}$, where the off-diagonal elements are zero and the excited state probability is typically much smaller in comparison with the modulated case. Thus, the analysis of the two-level system steady state shows the enhanced interaction due to the modulation of the free electron.

Before reaching the steady state, the two-level system may experience Rabi oscillation if $T < 8|gs|\tau$, which can be observed with state-of-the-art experimental technology (Supplemental Material, Sec. VII [29]). In the limit of small two-level-system decay rate, the Rabi oscillation frequency is $\Omega_R = 2|gs|/T$, which is consistent with the semiclassical results [25]. The physical intuition about this consistency is that the classical interpretation of $s = \langle b \rangle$ is the amplitude of the current distribution with spatial frequency $k = \omega_a/v_0$ [15]. Therefore, our theory provides a rigorous foundation for the semiclassical results.

Conclusion.—We present a quantum description for the interaction between a free electron and a two-level system that reveals the quantum entanglement and applies to the modulated electron straightforwardly. We highlight the enhancement of interaction due to the modulation of the free-electron wave function, which can be utilized to probe the atomic coherence. Such enhancement persists when the two-level system interacts with a dilute modulated electron beam. We also discuss an approach to create entanglement between distant two-level systems through the interaction with the same free electron. Our study of the free-electron–bound-electron interaction emphasizes the significance of free-electron wave function engineering and provides new perspectives for ultrafast physics studies using the free-electron probe.

We thank Prof. Meir Orenstein, Mr. Dylan Black, Dr. Jean-Philippe MacLean, Ms. Alison Rugar, Dr. Rahul Trivedi, Fan group members and members of the ACHIP Collaboration for helpful discussions and suggestions. This work is supported by the Gordon and Betty Moore Foundation (GBMF4744). Z.Z. acknowledges a Stanford Graduate Fellowship. X.-Q. S. acknowledges support from the Gordon and Betty Moore Foundation EPiQS Initiative through Grant No. GBMF8691.

Note added.—Recently, several papers [42–45] appeared on the preprint archive, providing quantum treatments of interactions of modulated electrons with the atom.

* xiaoqi20@illinois.edu

† shanhui@stanford.edu

- [1] A. H. Zewail, *Science* **328**, 187 (2010).
- [2] F. J. García de Abajo, *Rev. Mod. Phys.* **82**, 209 (2010).
- [3] A. Polman, M. Kociak, and F. J. G. de Abajo, *Nat. Mater.* **18**, 1158 (2019).
- [4] V. Di Giulio, M. Kociak, and F. J. G. de Abajo, *Optica* **6**, 1524 (2019).
- [5] V. U. Nazarov, *Phys. Rev. B* **59**, 9866 (1999).
- [6] V. U. Nazarov, V. M. Silkin, and E. E. Krasovskii, *Phys. Rev. B* **93**, 035403 (2016).
- [7] V. U. Nazarov, V. M. Silkin, and E. E. Krasovskii, *Phys. Rev. B* **96**, 235414 (2017).
- [8] B. Barwick, D. J. Flannigan, and A. H. Zewail, *Nature (London)* **462**, 902 (2009).
- [9] F. J. García de Abajo, A. Asenjo-Garcia, and M. Kociak, *Nano Lett.* **10**, 1859 (2010).
- [10] S. T. Park, M. Lin, and A. H. Zewail, *New J. Phys.* **12**, 123028 (2010).
- [11] A. Feist, K. E. Echternkamp, J. Schauss, S. V. Yalunin, S. Schäfer, and C. Ropers, *Nature (London)* **521**, 200 (2015).
- [12] K. E. Priebe, C. Rathje, S. V. Yalunin, T. Hohage, A. Feist, S. Schäfer, and C. Ropers, *Nat. Photonics* **11**, 793 (2017).
- [13] R. Dahan, S. Nehemia, M. Shentcis, O. Reinhardt, Y. Adiv, K. Wang, O. Beer, Y. Kurman, X. Shi, M. H. Lynch *et al.*, [arXiv:1909.00757](https://arxiv.org/abs/1909.00757).
- [14] O. Reinhardt and I. Kaminer, *ACS Photonics* **7**, 2859 (2020).
- [15] N. Rivera and I. Kaminer, *Nat. Rev. Phys.* **2**, 538 (2020).
- [16] G. M. Vanacore, I. Madan, G. Berruto, K. Wang, E. Pomarico, R. Lamb, D. McGrouther, I. Kaminer, B. Barwick, F. J. G. de Abajo *et al.*, *Nat. Commun.* **9**, 2694 (2018).
- [17] G. M. Vanacore, G. Berruto, I. Madan, E. Pomarico, P. Biagioni, R. Lamb, D. McGrouther, O. Reinhardt, I. Kaminer, B. Barwick, H. Larocque, V. Grillo, E. Karimi, F. J. García de Abajo, and F. Carbone, *Nat. Mater.* **18**, 573 (2019).
- [18] K. E. Echternkamp, A. Feist, S. Schäfer, and C. Ropers, *Nat. Phys.* **12**, 1000 (2016).
- [19] Y. Pan and A. Gover, *Phys. Rev. A* **99**, 052107 (2019).
- [20] R. Remez, A. Karnieli, S. Trajtenberg-Mills, N. Shapira, I. Kaminer, Y. Lereah, and A. Arie, *Phys. Rev. Lett.* **123**, 060401 (2019).
- [21] H. Larocque, I. Kaminer, V. Grillo, R. W. Boyd, and E. Karimi, *Nat. Phys.* **14**, 1 (2018).
- [22] I. Madan, G. M. Vanacore, S. Gargiulo, T. LaGrange, and F. Carbone, *Appl. Phys. Lett.* **116**, 230502 (2020).
- [23] J. Zhou, I. Kaminer, and Y. Pan, [arXiv:1908.05740](https://arxiv.org/abs/1908.05740).
- [24] L. Favro, D. Fradkin, and P. Kuo, *Phys. Rev. D* **3**, 2934 (1971).
- [25] A. Gover and A. Yariv, *Phys. Rev. Lett.* **124**, 064801 (2020).
- [26] D. Rätzel, D. Hartley, O. Schwartz, and P. Haslinger, [arXiv:2004.10168](https://arxiv.org/abs/2004.10168).
- [27] O. Kfir, *Phys. Rev. Lett.* **123**, 103602 (2019).
- [28] R. Ritchie and A. Howie, *Philos. Mag. A* **58**, 753 (1988).
- [29] See Supplemental Material at <http://link.aps.org/supplemental/10.1103/PhysRevLett.126.233402> for (i) detailed derivation of the electron-atom scattering matrix with relativistic correction, (ii) coupling coefficient for SnV, (iii) PINEM modulated Gaussian electron wave packet, (iv) optimal PINEM modulation for measuring the atomic coherence, (v) discussion of experimental realization, (vi) details of entangling 2 atoms with an electron, and (vii) discussion of interaction between an atom and a dilute electron beam, which includes Refs. [30–34].
- [30] R. C. Hilborn, *Am. J. Phys.* **50**, 982 (1982).
- [31] Y. Yang, A. Massuda, C. Roques-Carnes, S. E. Kooi, T. Christensen, S. G. Johnson, J. D. Joannopoulos, O. D. Miller, I. Kaminer, and M. Soljačić, *Nat. Phys.* **14**, 894 (2018).
- [32] F. W. Olver, D. W. Lozier, R. F. Boisvert, and C. W. Clark, *NIST Handbook of Mathematical Functions Hardback and CD-ROM* (Cambridge University Press, Cambridge, England, 2010).
- [33] J. McNeur, M. Kozak, D. Ehberger, N. Schönenberger, A. Tafel, A. Li, and P. Hommelhoff, *J. Phys. B* **49**, 034006 (2016).
- [34] A. Ceballos, Silicon photocathodes for dielectric laser accelerators, Ph. D. thesis, Doctoral dissertation, Stanford University, 2019.
- [35] M. E. Trusheim, B. Pingault, N. H. Wan, M. Gündoğan, L. De Santis, R. Debroux, D. Gangloff, C. Purser, K. C. Chen, M. Walsh, J. J. Rose, J. N. Becker, B. Lienhard, E. Bersin, I. Paradeisanos, G. Wang, D. Lyzwa, A. R.-P. Montblanch, G. Malladi, H. Bakhru, A. C. Ferrari, I. A. Walmsley, M. Atatüre, and D. Englund, *Phys. Rev. Lett.* **124**, 023602 (2020).
- [36] A. E. Rugar, C. Dory, S. Aghaeimeibodi, H. Lu, S. Sun, S. D. Mishra, Z.-X. Shen, N. A. Melosh, and J. Vučković, [arXiv:2005.10385](https://arxiv.org/abs/2005.10385).
- [37] D. S. Black, U. Niedermayer, Y. Miao, Z. Zhao, O. Solgaard, R. L. Byer, and K. J. Leedle, *Phys. Rev. Lett.* **123**, 264802 (2019).

- [38] N. Schönenberger, A. Mittelbach, P. Yousefi, J. McNeur, U. Niedermayer, and P. Hommelhoff, *Phys. Rev. Lett.* **123**, 264803 (2019).
- [39] Y. Morimoto and P. Baum, *Nat. Phys.* **14**, 252 (2018).
- [40] J.D. Cox and F.J. García de Abajo, *Nano Lett.* **20**, 4792 (2020).
- [41] F. P. Laussy, E. del Valle, and C. Tejedor, *Phys. Rev. B* **79**, 235325 (2009).
- [42] R. Ruimy, A. Gorlach, C. Mechel, N. Rivera, and I. Kaminer, following Letter, *Phys. Rev. Lett.* **126**, 233403 (2021).
- [43] A. Gover, B. Zhang, D. Ran, R. Iancu, A. Friedman, J. Scheuer, and A. Yariv, [arXiv:2010.15756](https://arxiv.org/abs/2010.15756).
- [44] L. J. Wong, N. Rivera, C. Murdia, T. Christensen, J. D. Joannopoulos, M. Soljačić, and I. Kaminer, *Microscopy* **37**, 47 (2020).
- [45] F. de Abajo and V. Di Giulio, [arXiv:2010.13510](https://arxiv.org/abs/2010.13510).